

# The Growth of Baryonic Structure in the presence of Cosmological Magnetic Pressure

Lorena Gazzola<sup>\*</sup>, Emma J. King, Frazer R. Pearce & Peter Coles

*School of Physics & Astronomy, University of Nottingham, University Park, Nottingham, NG7 2RD*

19 October 2018

## ABSTRACT

We follow the growth of baryonic structure in the presence of a magnetic field within an approximate cosmological magneto-hydrodynamic simulation, produced by adding an (isotropic) magnetic pressure related to the local gas pressure. We perform an ensemble of these simulations to follow the amplification of the field with time. By using a variety of initial field strengths and changing the slope of the power law that governs the way the field grows with increasing density we span the range of current observations and demonstrate the size of the effect realistic magnetic fields could have on the central density of groups and clusters. A strong magnetic field significantly reduces the central gas density which, in turn, reduces observable quantities such as the X-ray luminosity.

**Key words:** magnetic fields, hydrodynamics, methods: numerical, galaxies: clusters: general

## 1 INTRODUCTION

In an era where we have such a firm grasp of many of the fundamental parameters that define the universe in which we live (Spergel *et al.* 2003), the underlying framework of cosmology based on gravitational instability of cold dark matter is no longer subject to serious doubt. However, although the idea that large potential wells are built up by the hierarchical assembly of many thousands of smaller sub-blocks (Press & Schechter 1974; Davis *et al.* 1985) has not been seriously challenged for decades, there is much current debate about the presence or absence of large amounts of sub-structure (Kazantzidis *et al.* 2004) and about the cuspieness of the inner parts of dark matter profiles (Moore *et al.* 1999; Power *et al.* 2003; Diemand, Moore & Stadel 2004). Moreover, the reaction of baryonic material to this underlying framework is not well understood at all. We still do not readily understand why such a small fraction of baryons cools to form stars (Fukugita, Hogan & Peebles 1998; Balogh *et al.* 2001), how the first stars are distributed (Abel, Bryan & Norman 2002) and subsequently reionize the universe (Sokasian *et al.* 2004) or why the gas at the centre of dark matter haloes obstinately refuses to cool efficiently (Ponman *et al.* 1999; Pearce *et al.* 2000, 2001; Voit & Bryan 2001).

An additional complication arises from the well-known fact that the intra-cluster medium (ICM) in galaxy clusters is magnetized. This is inferred from observations of diffuse radio haloes and hard X-ray emission as well as Faraday rotation measurements (Kronberg 1994; Feretti & Giovannini 1996; Govoni *et al.* 2001a; Taylor *et al.* 2001; Eilek & Owen 2002; Murgia *et al.* 2004; Fusco-Femiano *et al.* 2004). Magnetic fields are observed throughout the Universe at a wide range of epochs and scales; from a few  $\mu G$  up to a few  $mG$  within galaxies (Beck 2000; Krause 2003), and from a few tenths of a  $\mu G$  on cluster and super-cluster scales, to values in the centre of cooling flow clusters reaching as high as a few tens of  $\mu G$  (Carlstrom, Holder & Reese 2002). At high redshifts magnetic fields of a few  $\mu G$  have been observed in systems such as Lyman- $\alpha$  absorption systems, (Kronberg & Perry 1982; Norman 1990; Kronberg 1994; Oren & Wolfe 1995), radio-galaxies (Athreya *et al.* 1998; Pentericci *et al.* 2000), and proto-clusters (Pentericci *et al.* 2000; Bagchi *et al.* 2002). Although magnetic fields of the order of  $\mu G$  in strength may seem insignificant, the vast scales involved mean that a significant amount of energy is stored in these fields, and consequently they can be dynamically important. Where they come from is still a mystery. In this paper we shall assume that some primordial seed field exists and experimentally determine whether it can have a significant effect on cluster properties.

Analytical and numerical studies provide an impor-

<sup>\*</sup> E-mail: ppxlg@nottingham.ac.uk

tant counterpoint to these observations, aiding our understanding of the distribution and perhaps origin of the magnetic field. The first attempt to implement MHD (magneto-hydrodynamics) into SPH (smoothed particle hydrodynamics) was the polytropes studied by Gingold & Monaghan (1977). Further aspects of the application of SPH to magnetic phenomena were considered by Phillips & Monaghan (1985), Phillips (1986) and Monaghan (1992). Phillips & Monaghan demonstrated that when the MHD equations are written in a conservative form a numerical effect occurs: SPH particles tend to clump due to the presence of an artificial tension. Subsequent authors (Meglicki, Wickramasinghe & Dewar 1995; Cerqueira & de Gouveia Dal Pino 2001; Hosking 2002) circumvented this problem using non-conservative forces but this approach does not work well when shocks are present. More recently, Price & Monaghan (2004) developed a new approach in which they added a small artificial stress that prevented the numerical instability.

Detailed MHD simulations of the growth of structure in the universe pointed out the importance of merger events on the distribution and strength of the final magnetic field and that the initial field structure is completely wiped out during cluster formation. In addition, compression and shear flows can strongly amplify the seed field (Birk, Wiechen & Otto 1999; Roettiger, Stone & Burns 1999; Dolag, Bartelmann & Lesch 1999, 2002).

Loeb & Mao (1994) have suggested that, if the resultant magnetic field were sufficiently strong, the ICM could be supported to a significant extent by magnetic pressure in addition to thermal gas pressure. In clusters where this was the case the magnetic field would be dynamically important (Dolag *et al.* 2001; Eilek & Owen 2002), so this support might contribute to the discrepancy between X-ray and gravitational lensing mass estimates of the central regions of galaxy clusters. Gonçalves & Friaça (1999) found that the magnetic field could be dynamically important on scales as small as  $\leq 1$  kpc, although it seems unlikely that either these small scale fields or a more widely distributed field such as that proposed by Loeb & Mao could be the main reason for the discrepancy between the mass estimates in the central regions, at least in relaxed clusters (Dolag *et al.* 1999; Dolag & Schindler 2000).

In this paper we examine the effect of introducing a large-scale magnetic field on the growth of baryonic structure. As gas collapses isotropically the magnetic field strength grows as  $B \propto \rho^{\frac{2}{3}}$  assuming that the field lines are frozen into the plasma. Accordingly, since the magnetic pressure is  $P_{\text{mag}} \propto B^2$ , the additional gas pressure due to the presence of a magnetic field rises as  $\rho^{\frac{4}{3}}$ . Here we implement this simple assumption into an  $N$ -body hydrodynamics code and follow what happens to the density of each of the gas particles. Obviously this method relies on a smooth collapse of the gas without massive tangling of the magnetic field lines, a situation that restricts its applicability to relatively low values of the overdensity. For this reason we have made no attempt to follow gas cooling or galaxy formation, but have concentrated on the hot haloes of

galaxy groups and clusters. In order to mimic more realistic fields we parametrise our model so that the power-law index for the  $B - \rho$  relation is one of the free parameters,  $\alpha$ ; the motivation for this is discussed in the next section, where we detail our numerical models and magnetic field approximation. Our results are presented in Sections 3 & 4, where we study various initial field strengths and power law dependencies with density as well as varying the redshift at which the field is initiated. Section 5 contains a discussion and our conclusions.

## 2 NUMERICAL CALCULATIONS

### 2.1 The Simulation Method

The basis for our model of the passive evolution of magnetic fields is Hydra, an  $AP^3M - SPH$  code (Couchman, Thomas & Pearce 1995). Smoothed-particle Hydrodynamics (SPH) is a Lagrangian numerical method which follows the motion of a set of fluid (gas) elements represented by discrete particles. The thermal energy and velocity of each particle are known at any given time and each particle has a fixed mass. Properties of the gas at the position of a particle can be estimated by smoothing these quantities over the  $N_{\text{SPH}}$  nearest neighbouring particles. The gas properties are then used to calculate the forces acting on each particle in order to update the positions and velocities. In cosmological simulations both dark matter and gas particles are included and the particles are initially distributed in a manner consistent with a cosmological power spectrum. If the process of galaxy formation is to be simulated then radiative cooling of the gas must also be included; we neglect this for the purposes of this paper.

The base simulation used throughout this paper has  $128^3$  gas and  $128^3$  dark matter particles with individual masses of  $6.58 \times 10^8 h^{-1} M_{\odot}$  and  $4.27 \times 10^9 h^{-1} M_{\odot}$  respectively, in a periodic box of  $50 h^{-1} \text{Mpc}$ . The power spectrum is that appropriate to a cold dark matter universe with the following parameter values: mean mass density parameter  $\Omega_M = 0.3$ , cosmological constant  $\Omega_{\Lambda} = 0.7$ , baryon density parameter  $\Omega_b = 0.04$ , Hubble constant (in units of  $100 \text{kms}^{-1} \text{Mpc}^{-1}$ ),  $h = 0.7$ , power spectrum shape parameter  $\Gamma = 0.21$  and rms linear fluctuation amplitude  $\sigma_8 = 0.90$ . These cosmological parameters are close to those obtained through fits to *WMAP* data (Spergel *et al.* 2003):  $\Omega_M = 0.27$ ,  $\Omega_{\Lambda} = 0.73$ ,  $\Omega_b = 0.044$ ,  $h = 0.71$ ,  $\sigma_8 = 0.84$ . The gravitational softening length is  $20 h^{-1} \text{kpc}$ , fixed in physical coordinates. The starting redshift was  $z_{\text{start}} = 49$ .

We carried out a set of 9 runs, each one characterised by different parameter values (see Table 1 and following section). For each run we extracted clusters with a spherical overdensity criteria and selected those with at least  $N = 1000$  particles of each kind within the virial radius. The number of objects we analysed is of the order of 140 per run. Given the limited volume of our simulations, we have only a couple of moderately rich objects, with  $M_{\text{vir}} > 10^{14} h^{-1} M_{\odot}$ .

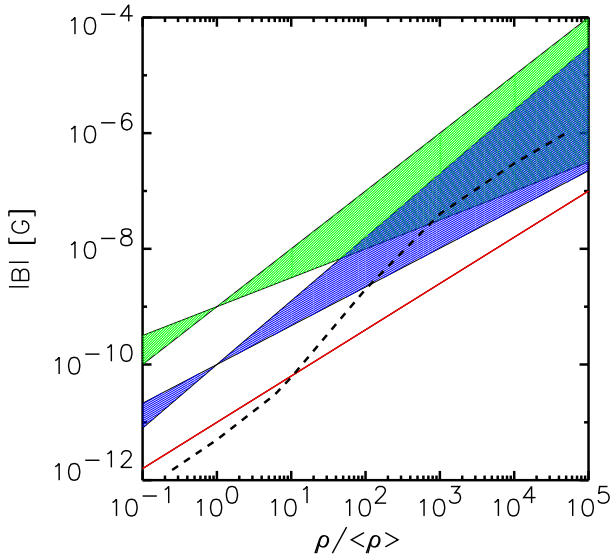


**Figure 1.** Magnetic field strength as a function of overdensity. The shaded regions and the continuous line delimit our range of  $\alpha$  and  $B_0$ . Top green:  $B_0 = 10^{-9}G$  and  $0.5 \leq \alpha \leq 1.1$ ; bottom blue:  $B_0 = 10^{-10}G$  and  $2/3 \leq \alpha \leq 1.1$ ; red continuous line:  $B_0 = 10^{-11}G$   $\alpha = 0.8$ . The black dashed line is from Dolag et al. 2005.

| Model | Field normalisation<br>$B_0$ [Gauss] | slope<br>$\alpha$ |
|-------|--------------------------------------|-------------------|
| noB   | 0                                    | -                 |
| B0960 | $10^{-9}$                            | 1.00              |
| B0948 | $10^{-9}$                            | 0.80              |
| B0940 | $10^{-9}$                            | 2/3               |
| B0930 | $10^{-9}$                            | 0.50              |
| B1066 | $10^{-10}$                           | 1.10              |
| B1060 | $10^{-10}$                           | 1.00              |
| B1048 | $10^{-10}$                           | 0.80              |
| B1040 | $10^{-10}$                           | 2/3               |
| B1148 | $10^{-11}$                           | 0.80              |

**Table 1.** Parameters for the simulations used in this paper. By column a simulation identifier, the magnetic field normalization in Gauss ( $B_0$ ) and the power law index of the field–density relation ( $\alpha$ ).

## 2.2 Approximating a Magnetic field

In this section we describe how we introduce a magnetic field into our simulations and justify our choice of parameters.

According to the standard picture of magnetic field evolution a seed field generated at high redshift is amplified by adiabatic compression and merger events occurring during cluster formation. A straightforward analytical argument shows that under the assumptions of:

- B-field frozen into plasma

- uniform spherical collapse
- small magnetic field
- mass conservation
- magnetic flux conservation,

then  $B$  scales with the gas density  $\rho$  as  $B \propto \rho^\alpha$  with  $\alpha = 2/3$ . On the other hand, if the magnetic field is important, there will be a preferential axis  $x$  for the collapse due to the presence of strong field lines and the collapse proceeds *cylindrically*. This, together with flux conservation and the assumption that gravity is in equilibrium with thermal pressure along the symmetry axis ( $2\pi G\rho x^2 \sim c_s^2$ ) leads to  $B \propto (T\rho)^{1/2}$ , so if the object is isothermal the power-law relation between  $B$  and  $\rho$  acquires a different value of  $\alpha = 1/2$  (Crutcher 1999).

More detailed numerical studies have found that in realistic large-scale structures without special geometries the amplification of the seed field is not quite as expected from these simple collapse models, with a rough power-law dependence but a higher value of  $\alpha$  (Roettiger et al. 1999; Dolag et al. 1999; Dolag et al. 2005). King & Coles (2006) showed that an average over small-scale collapses leads to an average value of  $\alpha$  which is higher than the isotropic value  $\alpha = 2/3$ ; the average of a non-linear function is not the same as the non-linear function of the average. Moreover, other phenomena such as mergers and anisotropies act to enhance the field still further. It is therefore likely that different power indices better describe the field behaviour in different density ranges, as found observationally: Dolag et al. (2001) found  $\alpha = 0.9$  for the galaxy cluster Abell 119, while Crutcher (1999) got  $\alpha = 0.47$  for molecular clouds in a density regime of about  $10^3 - 10^4 \text{cm}^{-3}$ .

The parametrisation we have chosen corresponds to a polytropic equation of state of the form  $P \propto \rho^{2\alpha}$ ; large values of  $\alpha$  will therefore produce a steeper relation than pertains for the thermal pressure ( $\alpha \simeq 5/6$ ). This is the regime in which interesting physics can occur.

These considerations all lead us to approximate the magnetic field  $B(z)$  as:

$$B(z) = B_0(1+z)^{3\alpha}\rho^\alpha, \quad (1)$$

where  $\rho$  is the local overdensity,  $B_0$  the field in an unperturbed universe, both in comoving units, and  $z$  is the redshift. The term  $\rho^\alpha$  accounts for the field amplification by incorporating  $\alpha$  as a free parameter. By varying the power-law index we emulate the different possible amplification mechanisms, though we stress that we do not solve the full MHD equations exactly, in particular we ignore the back-reaction of the field on the gas which would break the simple scaling of equation (1). In reality it is likely that the amplification of a  $B$ -field by the factors we have discussed would saturate around the equipartition value. Care must be taken, therefore, in interpreting our results when magnetic pressure dominates the thermal pressure. We are primarily interested, however, in the growth of structures through the linear and quasi-linear regime so we hope our calculations have a reasonable regime of validity. It is also important to understand that we can not use this method to simulate ordered fields displaying large-scale anisotropy: we are restricted to fields that are tangled on a sufficiently

small scale that their effect on the large-scale gas motion is isotropic.

The standard SPH momentum equation for particle  $i$  using a smoothing kernel  $W$  is:

$$\frac{d\vec{v}_i}{dt} = - \sum_j m_j \left( \frac{P_i}{\rho_i^2} + \frac{P_j}{\rho_j^2} + \prod_{ij} \right) \nabla_i W_{ij}, \quad (2)$$

and the corresponding equation for the rate of change of the internal energy  $e_i$  is

$$\frac{de_i}{dt} = \frac{1}{2} \sum_j m_j \left( \frac{P_i}{\rho_i^2} + \frac{P_j}{\rho_j^2} + \prod_{ij} \right) \vec{v}_{ij} \cdot \nabla_i W_{ij}, \quad (3)$$

where  $\vec{v}_{ij}$  is the relative momentum of particles  $i$  and  $j$ . In these equations  $P_i$  is the pressure measured at the position of the  $i$ -th particle.

Given the presence of a magnetic field, the magnetic contribution to the pressure can be written as

$$P_{\text{mag}} = \frac{B^2}{2\mu_0}, \quad (4)$$

with  $\mu_0 = 4\pi \times 10^{-7}$  and  $B$  is interpreted as the *rms* value of the (tangled) field. If we assume that the magnetic field is passively moved and squeezed by the gas we can think of this magnetic pressure as being related to the baryonic density in the same way as the thermal pressure but with a different equation of state described by the parameter  $\alpha$ . Writing  $P = P_{\text{th}} + P_{\text{mag}}$  where  $P_{\text{th}}$  is the thermal pressure (calculated using the standard SPH methods) we can accommodate both forms in the standard SPH equations by simply adding an extra effective pressure variable. Note, however that this approach has severe limitations: there is no back-reaction of the field on the gas; it cannot cope with large-scale magnetic structures which are inherently anisotropic; and the polytropic model we use does not rigorously conserve energy. One should not place too much literal emphasis on the quantitative results we present, especially for high densities.

The magnetic field strength as a function of over-density at  $z = 0$  in our models is shown in Figure 1. We fixed the normalization factor  $B_0$  and the power law index  $\alpha$  so that we span the range of observed field strengths in halo cores as well as the values obtained by the more complex model of Dolag *et al.* (2005) which is shown as the dashed line. The top green shaded region represents the area in the  $B$ - $\rho$  plane where  $B_0 = 10^{-9}G$  and  $0.5 \leq \alpha \leq 1$ .; the lower blue region is relative to  $B_0 = 10^{-10}G$  and  $2/3 \leq \alpha \leq 1.1$  while the red continuous line is  $B_0 = 10^{-11}G$  and  $\alpha = 0.8$ .

For these values the highest normalisation models challenge the latest observational constraints for the magnetic energy density in clusters obtained from Faraday rotation measures (Vogt & Ensslin, 2006). Our models were chosen to span the full range of possible magnetic field strengths, with the strongest fields larger than observed (and so producing consequences larger than expected in the observed Universe).

In uncollapsed regions the observed strength of the magnetic field is currently only an upper limit. Sev-

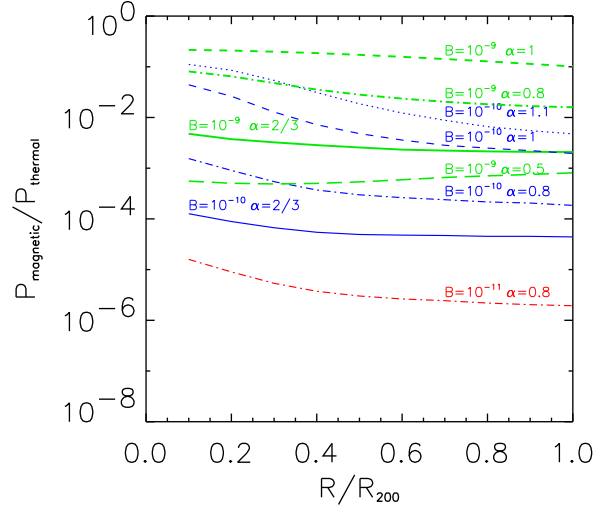


**Figure 2.** Mean radial fractional pressure. Each line represents a different run with the parameters labelled and displays the mean ratio of the thermal to magnetic pressure in concentric spherical bins over all clusters.

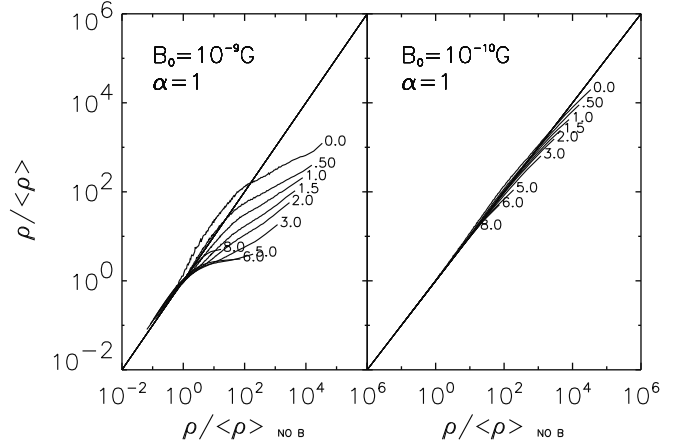


**Figure 3.** A comparison at different redshifts of the densities of equivalent gas particles from simulations without a magnetic field (noB) and one with a magnetic field of strength  $10^{-9}G$ ,  $\alpha = 1$ . (B0960, left panel) and a magnetic field of strength  $10^{-10}G$ ,  $\alpha = 1$ . (B1060, right panel). The appropriate redshift is labelled at the end of each profile.

eral of our power-law models exceed this value but as no structures collapse and we are not analysing these volumes this has no affect on our results. Our weakest field strength was chosen so as to fall within the range of allowed values in the voids.

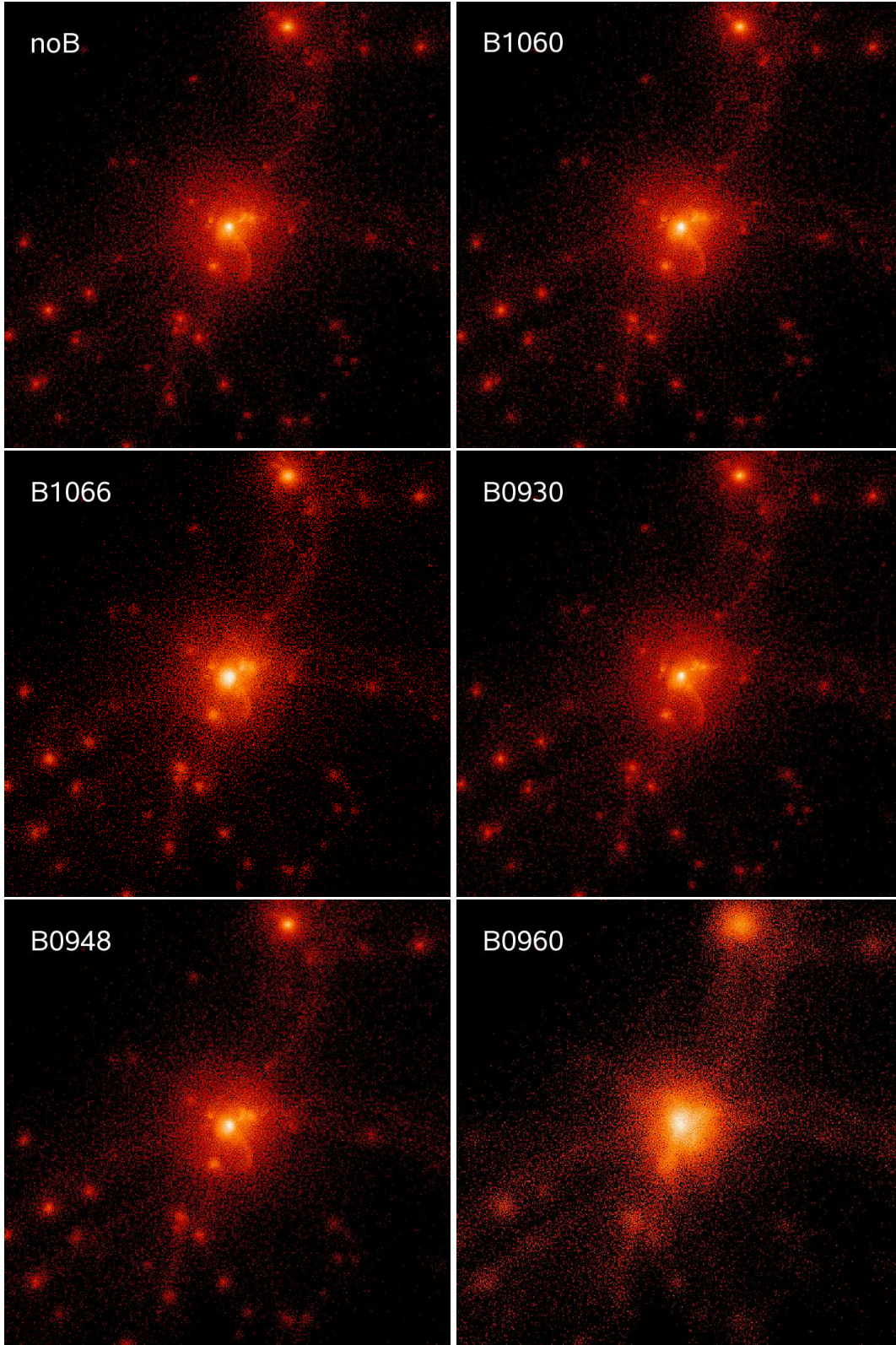


**Figure 4.** Mass maps at  $z = 0$  for noB, B1060, B1066 (left, top to bottom); B0930, B0948 and B0960 (right, top to bottom). The box side is  $10h^{-1}\text{Mpc}$  and the central object has a mass of  $1.5 \times 10^{14}h^{-1}M_{\odot}$ .

Once the amplitude and power-law index of the magnetic field have been chosen there remains the choice of the redshift at which the field is first imposed. If the magnetic field is turned on at late times, after much of the structure has formed, then it has little effect on the resultant objects. If, however, the field is imposed before significant structures form (which in turn depends on the resolution of the particular simulation being studied) then the initial redshift makes little difference to the final distribution of the matter.

Using trial simulations we established that for reasonable choices of initial field,  $z \geq 5$  is necessary to have significant effect, but at higher redshifts the specific choice of  $z$  is not important. We therefore impose the magnetic field at  $z = 9$  for all subsequent runs.

### 3 REDSHIFT EVOLUTION

We start our analysis with Figure 2 where we show the ratio of  $P_{\text{mag}}$  versus  $P_{\text{th}}$  as a function of radii. The values have been obtained averaging over all clusters and each line is relative to a different run. The inclusion of a magnetic field  $B$  adds a non-thermal pressure  $P_{\text{mag}} \propto B^2$  that counteracts gravity. When  $P_{\text{mag}}$  is not negligible compared to  $P_{\text{th}}$  the magnetic fields become dynamically important in that the additional magnetic pressure supports the gas against gravity and so for the same temperature the gas can reside at a lower density. Also, the additional pressure can slow the infall of the gas, retarding the evolution of structure. In reality we found that  $P_{\text{mag}}$  is orders of magnitude smaller than  $P_{\text{th}}$  in most cases and the ratio of gas magnetic to thermal pressure generally falls with radius. However, even an additional 1% pressure support in the core region of collapsed objects can have serious consequences, particularly for observables such as the X-ray luminosity which depends on the square of the gas density.

In Figure 3 we plot the rank-ordered density of all the particles in the run with magnetic field compared to the rank ordered density without a magnetic field at a range of different redshifts. With the larger field (left panel) the high density particles incur an appreciable drop in their density. At lower field values (right panel) the effect of the magnetic field is much reduced.

As can be seen for the high field redshift zero case, at low redshifts and high field values particles near the mean density actually end up denser than when no magnetic field was present. This is due to the magnetic field pressure slowing the infall and reducing the strength of the accretion shock, resulting in a lower final entropy and consequently greater final density. We find that 70% of the particles with density ratio  $\rho_{0960}/\rho_{\text{noB}} > 1$  have entropy ratio  $s_{0960}/s_{\text{noB}} < 1$ , while the percentage increases to more than 90% if we consider particles with  $\rho_{0960}/\rho_{\text{noB}} > 10$  (where  $\rho_{0960}$  ( $s_{0960}$ ) and  $\rho_{\text{noB}}$  ( $s_{\text{noB}}$ ) are the densities (entropies) for run 0960 and noB).

In Figure 4 we show a series of gas density maps (where brighter colours indicates denser gas) of a box of side  $10h^{-1}\text{Mpc}$  centered on one of the most massive clusters ( $1.5 \times 10^{14}h^{-1}M_{\odot}$ ). In this sequence of 6 panels the field strength generally increases down the page

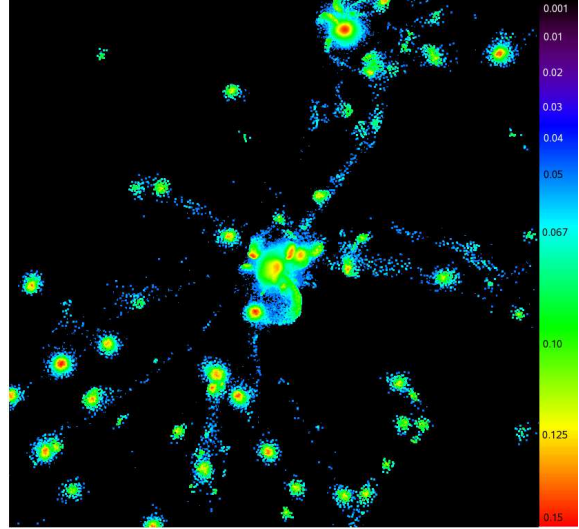


**Figure 5.** Map of the ratio of magnetic to thermal pressure at  $z = 0$  for B1060. The box is  $10h^{-1}\text{Mpc}$  across, same region as in figure 4.

with the precise configuration of the magnetic field formulation that corresponds to each panel given in Table 1. The presence of a strong magnetic field also results in a smoother mass distribution, with small clumps washed out and less frequent shocks.

Spatially mapping the ratio of the magnetic to thermal pressure as in Figure 5 (which shows the same region as in Figure 4) reveals that only in small objects and cluster cores can the magnetic pressure approach equipartition with the thermal pressure ( $P_{\text{mag}} \sim 0.1 - 0.3P_{\text{th}}$ ), provided that  $B_0$  and  $\alpha$  are sufficiently high ( $B_0 \geq 10^{-10}$  and  $\alpha \geq 1$ ). This results in a shallower density profile (Figure 6) and a lower entropy level in the inner regions of collapsed objects, while the outskirts are not affected. The mean radial gas density profile is displayed in Figure 6 which shows that field strengths not much higher than those observed can significantly depress the central gas density. Moreover we expect small structures to be affected more than big clusters because the former are characterised by a shallow gravitational potential and so a relatively small additional pressure can be sufficient to deter gas infall. This can be easily seen from density maps (Figure 4) but, due to the small simulation volume, we do not have a wide range in mass to properly address any trend in mass from density profiles. Also, unfortunately, our spatial resolution is not high enough to properly investigate the regions where the magnetic field effects should be more pronounced. In Figure 7 we show the bolometric luminosity in  $\text{erg s}^{-1}$  versus the bolometric emission weighted temperature in KeV for different runs. The reduction in the central gas density lowers the bolometric X-ray luminosity of a group-size object ( $M < 10^{13}h^{-1}M_{\odot}$ ) by 40 – 70% for field values of  $B_0 = 10^{-10}G$  and  $\alpha = 1.1$  (Figure 7). The reduction in luminosity can be even more than one order of magnitude for the strongest field we analysed.

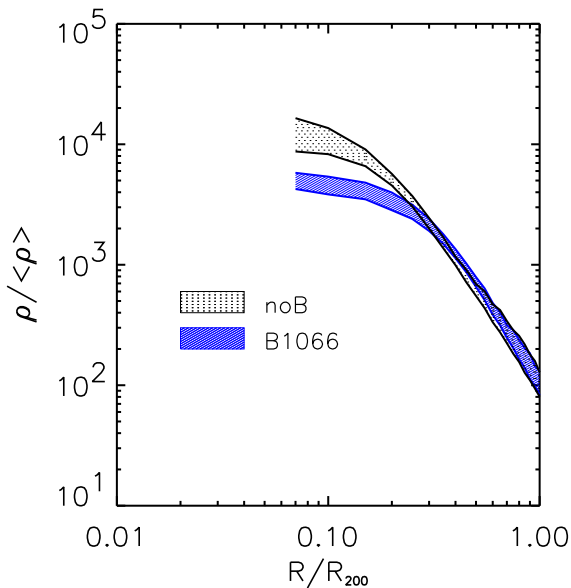


**Figure 6.** Density profile at  $z = 0$  for our clusters. The lines represent the first and the third quartile, the dashed blue area is for run B1066 and the white dotted one for the noB run.

#### 4 OBSERVATIONAL CONSEQUENCES

When considering densities typical of collapsed objects at  $z = 0$  we find that the average density profile of the haloes becomes shallower in the core and the core entropy level increases when a magnetic field is added to our simulations. On the other hand, the density profile in the outskirts is not affected, even in the presence of a strong field because it is mainly in the inner regions that the magnetic pressure can reach equipartition with the thermal pressure (see Figure 2), while in the outskirts it is always negligible. This shallowing of the gas density profile results in a more extended gas distribution and naturally leads to a reduction in the baryon fraction within our objects in the presence of a magnetic field (Figure 8) (see Ettori *et al.* (2006) for a wider discussion of this topic). For a reasonably high field strength and slope (run B0960) the baryon fraction is reduced to 60% of the cosmic value, with the effect becoming more dramatic as the halo mass decreases.

Figure 9 displays the ratio of the gas mass within  $r_{2500}$  (the radius that encloses an overdensity of 2500) for the models with various magnetic field strengths compared to the gas fraction obtained in the run without a magnetic field. For regions with overdensities exceeding 2500 times the mean (which corresponds to the halo core region which is typically well observed in X-rays) the baryonic mass fraction can be even more dramatically reduced, although the effect is only particularly pronounced for higher field strengths.

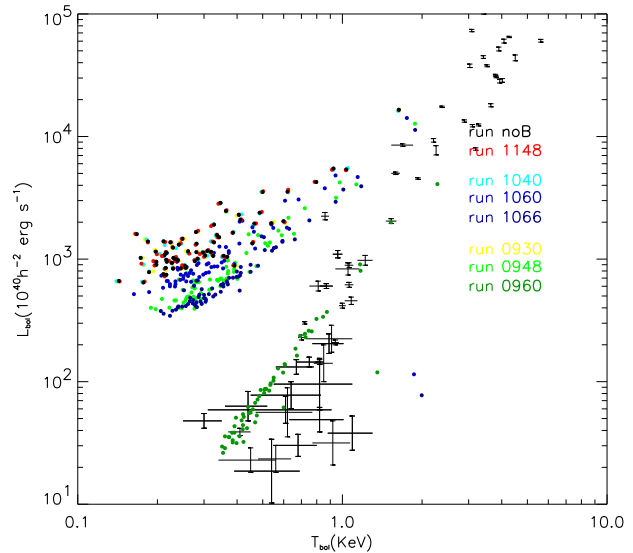


**Figure 7.** The luminosity–temperature relation. The values plotted are the emission weighted temperature and the bolometric luminosity within  $r_{500}$ . Observations are from Ponman *et al.* 1996; Helsdon *et al.* 2000 and Novicki *et al.* 2002.

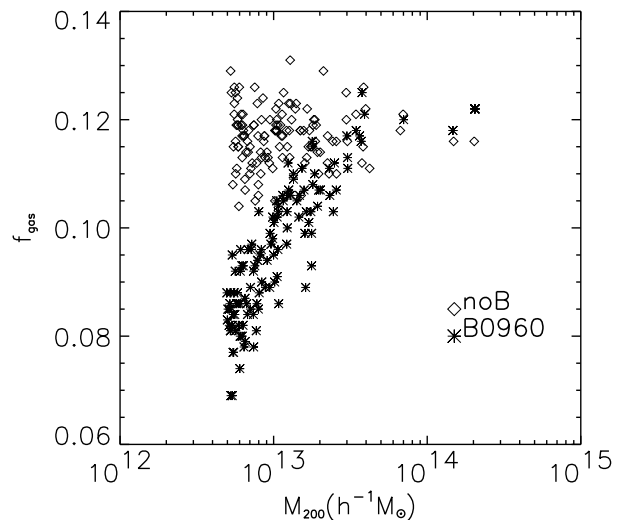


**Figure 8.** Gas fraction within the virial radius as a function of the virial mass at  $z = 0$  for a run with no magnetic field and with  $B_0 = 10^{-9}G$  and  $\alpha = 1$ .

#### 5 SUMMARY & CONCLUSIONS

We have presented a simple approximate scheme that implements an isotropic magnetic field within standard SPH. This method allows various field strength and amplification schemes to be quickly and efficiently tested. Using our approach we have modelled the full range of observed field strengths and shown that the stronger

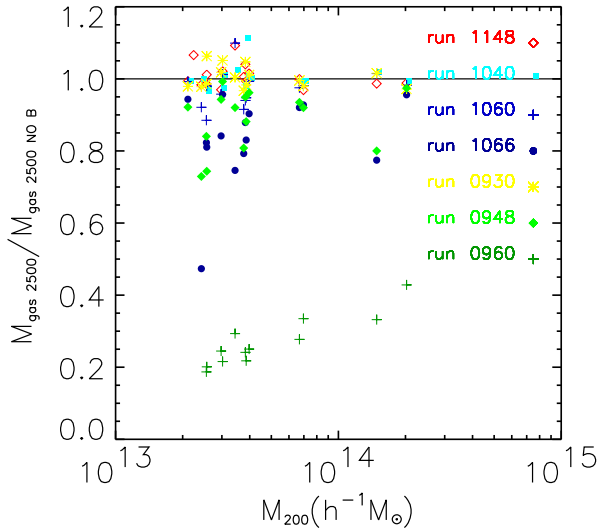


**Figure 9.** Relative gas mass within  $r_{2500}$  (the radius enclosing an overdensity of 2500) in runs with a magnetic field versus the total virial mass in the run without a magnetic field. The different symbols mark different runs.

fields can have a significant affect on the halo core regions.

It is important to note that this work could equally well be applied to any physical process that supplements the usual gas pressure support with additional pressure which has a power-law relationship to the density. This could include local turbulence (Dolag *et al.* 2006), the injection of hot gas from supernovae (Silich, Tenorio-Tagle & Anorve-Zeferino 2005), radio bubbles (Ensslin 2003; Soker & Pizzolato 2005; Fabian *et al.* 2006), or the activity of galactic nuclei (Sijacki & Springel 2006). As would perhaps have been expected smaller haloes are more significantly altered by these processes, particularly when there is a strong density dependence.

Any physical process that effects the central baryonic density within dark matter haloes is astrophysically interesting because such a process will naturally alter star formation rates, feeding of any central black hole and the global X-ray emission from the object (to name but a few). Even a small lowering of the central density can have a dramatic effect because many of these associated processes operate on a high power of the local density (for instance, the X-ray emission, largely due to thermal bremsstrahlung, is related to the density squared).

If it indeed turns out that large scale astrophysical magnetic fields are similar in strength to those suggested by Dolag *et al.* (2001) then in the main they will have little effect, particularly if they remain untangled and so amplify with the density to a low power. If the magnetic field in collapsed regions becomes tangled however, and so grows with a steeper power law dependence on density then their affects could be sig-

nificant, particularly within the very central regions of small haloes.

## ACKNOWLEDGEMENTS

We thank the referee for his thoughtful and detailed report which has allowed us to substantially improve the paper. LG acknowledges a University of Nottingham research studentship. The simulation work was performed on the Nottingham HPC facility.

## REFERENCES

- Abel T., Bryan G.L., Norman M.L., 2002, *Science*, 295, 93  
 Athreya R.M., Kapahi V.K., McCarthy P.J., van Breugel W., 1998, *A&A*, 329, 809  
 Bagchi J., Ensslin T.A., Miniati F., Stalin C.S., Singh M., Raychaudhury S., Humeshkar N.B., 2002, *New Astronomy*, 7, 249  
 Balogh M.L., Pearce F.R., Bower R.G., Kay S.T., 2001, *MNRAS*, 326, 1228  
 Beck R., 2000, *IAU joint discussion*, 14, 4  
 Birk G.T., Wiechen H, Otto, A., 1999, *ApJ*, 518, 177  
 Carlstrom J.E., Holder G.P., Reese E.D., 2002, *ARA&A*, 40, 643  
 Cerqueira A.H. & de Gouveia Dal Pino E.M., 2001, *ApJ*, 560, 779  
 Couchman H.M.P., Thomas P.A., Pearce F.R., 1995, *ApJ*, 452, 797  
 Crutcher R.M., 1999, *ApJ*, 520, 706  
 Davis M., Efstathiou G., Frenk C.S., White S.D.M., 1985, *ApJ*, 292, 371  
 Diemand J., Moore B., Stadel J., 2004, *MNRAS*, 353, 624  
 Dolag K., Bartelmann M., Lesch H., 1999, *A&A*, 348, 351  
 Dolag K., Bartelmann M., Lesch H., 2002, *A&A*, 387, 383  
 Dolag K., Grasso D., Springel V., Tkachev I., 2005, *JCAP*, 1, 5  
 Dolag K., Schindler S., 2000, *A&A*, 364, 491  
 Dolag K., Schindler S., Govoni F., Feretti L., 2001, *A&A*, 378, 777  
 Dolag K., Vazza F., Brunetti G., Tormen G., 2006, *MNRAS*, 364, 753  
 Eilek J.A., Owen F.N., 2002, *ApJ*, 567, 202  
 Ensslin T., 2003, *ASPC*, 301, 159  
 Ettori S., Dolag K., Borgani S., Murante G., 2006, *MNRAS*, 365, 102  
 Fabian A.C., Sanders J.S., Taylor G.B., Allen S.W., Crawford C.S., Johnstone R.M., Iwasawa K., 2006, *MNRAS*, 366, 417  
 Feretti, L., & Giovannini, G. 1996, in *Extragalactic radio sources*, ed. R. Ekers, C. Fanti, & L. Padrielli (Kluwer Academic, Publisher), *IAU Symp.*, 175, 333  
 Fukugita M., Hogan C. J., Peebles P. J. E., 1998, *ApJ*, 503, 518  
 Fusco-Femiano R., Orlandini M., Brunetti G., et al. 2004, *ApJ*, 602, L73  
 Gingold R.A., Monaghan J.J., 1977, *MNRAS*, 181, 375  
 Gonçalves D.R., Friaça A.C.S., 1999, *MNRAS*, 309, 651  
 Govoni F., Feretti L., Giovannini G., et al. 2001a, *A&A*, 376, 803  
 Helsdon, S. F., & Ponman, T. J. 2000a, *MNRAS*, 315, 356  
 Hosking J.G., 2002, *PhD thesis*, Cardiff Univ.  
 Kazantzidis S., Mayer L., Mastropietro C., Diemand J., Stadel J., Moore B., 2004, *ApJ*, 608, 663  
 King E.J., Coles P., 2006, *MNRAS*, 365, 1288  
 Krause M., 2003, *Acta Astronomica Sinica*, 44, 123  
 Kronberg P.P., 1994, *Nature*, 370, 179  
 Kronberg P.P., 1994 *Rep. Prog. Phys.* 57 325-382  
 Kronberg P.P., Perry J.J., 1982, *ApJ*, 263, 518  
 Loeb A., Mao S., 1994, *ApJ*, 435, 109  
 Meglicki Z., Wickramasinghe D., Dewar R.L., 1995, *MNRAS*, 272, 717  
 Monaghan, J.J., 1992, *ARA&A*, 30, 543



- Moore B., Quinn T., Governato F., Stadel J., Lake G., 1999, MNRAS, 310, 1147
- Murgia M., Govoni F., Feretti L., Giovannini G., Dallacasa D., Fanti R., Taylor G.B. and Dolag K. A&A 424, 429-446, 2004
- Norman C.A., 1990, Proceedings of the Enrico Fermi International School of Physics, ed J. Andouze & F Melchiorri, p. 29. North-Holland, Amsterdam.
- Novicki, M. C., Sornig, M., & Henry, J. P. 2002, AJ, 124, 2413
- Oren A.L., Wolfe A.M., 1995, ApJ, 445, 624
- Pentericci L., Van Reeve W., Carilli C.L., Rottgering H.J.A., Miley G.K., 2000, A&AS, 145, 121
- Pearce F.R., Thomas P.A., Couchman H.M.P., Edge, A.C., 2000, MNRAS, 317, 1029
- Pearce F.R., Jenkins A, Frenk C.S., White S.D.M., Thomas P.A., Couchman H.M.P., Peacock J.A., Efstathiou G., 2001, MNRAS, 326, 649
- Phillips G.J., Monaghan J.J., 1985, MNRAS, 216, 883
- Phillips G.J., 1986, MNRAS, 221, 571
- Ponman, T. J., Bourner, P. D. J., Ebeling, H., & Bohringer, H. 1996, MNRAS, 283, 690
- Ponman T.J., Cannon D.B., Navarro J.F., 1999, Nature, 397, 135
- Power C., Navarro J.F., Jenkins A., Frenk C.S., White S.D.M., Springel V., Stadel J., Quinn T., 2003, MNRAS, 338, 14
- Price D.J., Monaghan J.J., 2004, MNRAS, 348, 123
- Press W.H., Schechter P., 1974, ApJ, 187, 425
- Roettiger K., Stone J.M., Burns J.O., 1999, ApJ, 518, 594
- Sijacki D., Springel V., 2006, MNRAS, 366, 397
- Silich S., Tenorio-Tagle G., Anorve-Zeferino G. A., 2005, ApJ, 635, 1116
- Sokasian A., Yoshida N., Abel T., Hernquist L., Springel V., 2004, MNRAS, 350, 47
- bibitemsp06Soker N., Pizzolato F., 2005, ApJ, 622, 847
- Spergel D. N. *et al.*, 2003, ApJS, 148, 175
- Taylor G.B., Govoni F., Allen S., & Fabian A. C. 2001, MNRAS, 326, 2
- Vogt C., Enlin T. A., 2006, Astronomische Nachrichten, Vol.327, Issue 5/6
- Voit G.M., Bryan G.L., 2001, Nature, 414, 425